Loss of *Aif* function causes cell death in the mouse embryo, but the temporal progression of patterning is normal

Doris Brown*†‡, Benjamin D. Yu*†‡, Nicholas Joza§¶, Paule Bénit‖, Juanito Meneses††, Meri Firpo††, Pierre Rustin‖**, Josef M. Penninger§¶, and Gail R. Martin*‡‡**

Departments of *Anatomy, †Dermatology, and ††Obstetrics, Gynecology, and Reproductive Sciences, University of California, San Francisco, CA 94143; §Institute of Molecular Biotechnology of the Austrian Academy of Sciences, Dr. Bohr-Gasse 3, 1030 Vienna, Austria; ¶Departments of Immunology and Medical Biophysics, University of Toronto, Toronto, ON, Canada M5S 3G3; ‖Institut National de la Santé et de la Recherche Médicale, U676, F-75019 Paris, France; and **Faculté de Médecine Denis Diderot, Université Paris, IFR02, F-75005 Paris, France

Contributed by Gail R. Martin, May 12, 2006

Apoptosis-inducing factor (AIF) is an evolutionarily conserved, ubiquitously expressed flavoprotein with NADH oxidase activity that is normally confined to mitochondria. In mammalian cells, AIF is released from mitochondria in response to apoptotic stimuli and translocates to the nucleus where it is thought to bind DNA and contribute to chromatinolysis and cell death in a caspase-independent manner. Here we describe the consequences of inactivating *Aif* in the early mouse embryo. Unexpectedly, we found that both the apoptosis-dependent process of cavitation in embryoid bodies and apoptosis associated with embryonic neural tube closure occur in the absence of AIF, indicating that *Aif* function is not required for apoptotic cell death in early mouse embryos. By embryonic day 9 (E9), loss of *Aif* function causes abnormal cell death, presumably because of reduced mitochondrial respiratory chain complex I activity. Because of this cell death, *Aif* null embryos fail to increase significantly in size after E9. Remarkably, patterning processes continue on an essentially normal schedule, such that E10 *Aif* null embryos with only ≈1/10 the normal number of cells have the same somite number as their wild-type littermates. These observations show that pattern formation in the mouse can occur independent of embryo size and cell number.

apoptosis | cavitation | embryo patterning | somitogenesis | mitochondrial respiratory chain complex I

Cell death plays a key role in both disease states and normal development. One of the earliest events in mouse embryogenesis, formation of the proamniotic cavity, is an apoptosis-dependent process (1). As yet, little is known about the molecular mechanisms that regulate normal apoptosis in the mammalian embryo. Inactivation of individual genes in the caspase pathway, which are considered the primary effectors of cell death, does not appear to prevent the normal cell deaths in early embryogenesis (2). In contrast, inactivation of *Pcdc8*, the gene that encodes apoptosis-inducing factor (AIF), has been reported to block cavitation in embryoid bodies (3), an *in vitro* model for proamniotic cavity formation (1). These data suggested that *Aif* function is an essential mediator of normal apoptosis in early mouse embryogenesis.

AIF was first identified as a mitochondrial protein that can induce changes characteristic of apoptosis in isolated nuclei. The mouse and human *Aif* genes are X-linked and encode highly conserved proteins that share significant homology with bacterial NADH-oxidoreductases. In healthy cells, the ubiquitously expressed AIF protein is confined to mitochondria. However, after treatment with agents that induce apoptosis, AIF can be found in the cytosol and nucleus (4). Based on these and other data, it has been proposed that AIF has an electron acceptor/donor (oxidoreductase) function and a second, independent apoptogenic function (5). AIF thus has features in common with cytochrome *c*, which is involved in electron shuttling between respiratory chain (RC) complexes within mitochondria, and becomes an effector of cell death after release into the cytosol by apoptotic stimuli. However, whereas cytochrome *c* is thought to exert its apoptogenic effect in the cytosol by participating in the activation of the executioner caspases (6), AIF appears to exert its apoptogenic effect via direct interaction with DNA (5), thereby functioning via a caspase-independent pathway.

The hypothesis that AIF mediates cell death in the early embryo has not been tested genetically until now. An initial effort to produce *Aif* null mice by gene targeting was unsuccessful because male ES cells carrying an *Aif* null allele on their single X-chromosome failed to form chimeric mice after injection into host blastocysts. A potential explanation for this observation is that the presence of Aif^{-}/Y ES cells unable to undergo normal apoptosis prevented development of the chimeric embryos (3). Here, we explore the function of *Aif* in normal embryogenesis by using Aif^{flox}, a recently described *Aif* conditional null allele, in which exon 7 is flanked by *loxP* sites. Cre-mediated recombination therefore deletes nucleotides 694 to 778, thereby disrupting the reading frame (7). Our data provide evidence that *Aif* is not required for apoptosis at early stages of development and, instead, is required for cell survival beginning at approximately embryonic day 9 (E9). The cell death caused by loss of *Aif* function resulted in an intriguing phenotype that demonstrated that pattern formation in the mouse can occur independent of embryo size and cell number.

Results

***Aif* Function Is Not Required for Apoptosis in Embryoid Bodies or Early Mouse Embryos.** Previous studies of Aif^{-}/Y embryoid bodies had suggested that loss of *Aif* function would prevent proamniotic cavity formation (3). However, when $Aif^{flox/+}$ females were crossed to males homozygous for a β-actin (Ac)-*cre* transgene that functions efficiently at preimplantation stages of development (8), their β-Ac-$cre^{Tg/0}$;Aif^{flox}/Y (*Aif* null) progeny developed for several days beyond the stage of proamniotic cavity formation (7). One possible explanation for this finding is that even though Aif^{flox} was converted to $Aif^{\Delta ex7}$ in all cells before proamniotic cavity formation (by E3.5; data not shown), AIF produced before Aif^{flox} was inactivated might have persisted until approximately E5.0 and been sufficient to enable proamniotic cavity formation in *Aif* null embryos. To test this hypothesis, we analyzed embryos that inherited $Aif^{\Delta ex7}$, which we

Conflict of interest statement: No conflicts declared.

Abbreviations: Ac, actin; AIF, apoptosis-inducing factor; C*n*, complex *n*; E*n*, embryonic day *n*; RC, respiratory chain; som, somite stage.

‡D.B. and B.D.Y. contributed equally to this work.

‡‡To whom correspondence should be addressed. E-mail: gail.r.martin@ucsf.edu.

www.pnas.org/cgi/doi/10.1073/pnas.0603950103

obtained by crossing wild-type males to β-Ac-cre$^{Tg/0}$;*Aif*$^{flox/+}$ (*Aif* null heterozygous) females. Although most such females die during embryogenesis because approximately half their cells are *Aif* null due to random X-chromosome inactivation, a few survive and transmit the *Aif*$^{\Delta ex7}$ allele. Significantly, *Aif*$^{\Delta ex7}$/Y and wild-type progeny of this cross were morphologically similar at approximately E7.75 (Fig. 1*A*), demonstrating that embryos that never contain a functional *Aif* gene are still able to form a proamniotic cavity.

Although these data left open the possibility that the ability to cavitate might be because of persistence of maternal AIF protein produced in the oocyte before fertilization, they strongly suggested that *Aif* function is not required for proamniotic cavity formation during embryogenesis. To explore this issue further, we sought to determine whether *Aif* null blastocyst-derived ES cells that had undergone ≈20 doublings to dilute out any residual AIF protein would form embryoid bodies that cavitated. We therefore established new ES cell lines from the progeny of a cross between *Aif*$^{flox/flox}$ or *Aif*$^{flox/+}$ females and β-Ac-cre$^{Tg/Tg}$ males. From 48 blastocysts cultured, we obtained 32 ES cell lines, 14 of which carried a Y chromosome. Half of these male ES cell lines carried the recombined *Aif* (null) allele and contained no AIF protein (Fig. 1 *B* and *C*, and data not shown). The rate of cell proliferation was the same for all *Aif* null, heterozygous, and wild-type ES cell lines while they were being established and subsequently maintained in culture (data not shown).

We cultured several of these cell lines by using conditions under which ES cells can form simple embryoid bodies consisting of an outer layer of endodermal cells surrounding a core of undifferentiated ES cells. In such embryoid bodies, signals from the endodermal cells trigger cavitation, a process during which some of the core cells die and the remaining core cells reorganize into a pseudostratified epithelium surrounding the cavity produced by cell death (1). Three *Aif* null ES cell lines, each isolated from a different embryo, formed cavitated (cystic) embryoid bodies (Fig. 1 *D* and *E*). PCR analysis confirmed that cavitating embryoid bodies contained only *Aif* null cells (data not shown). These data demonstrate that *Aif* function is not essential for cavitation in embryoid bodies. The difference between these observations and the previous finding that cavitation was completely blocked in embryoid bodies produced by three *Aif*$^{-}$/Y ES cell lines (3) is most likely a function of the culture conditions used. In support of this hypothesis, it has been observed recently that under different culture conditions, embryoid bodies formed by one of the *Aif*$^{-}$/Y ES cell lines undergo at least partial cavitation, although they fail to completely clear the dead cells from the central core when cultured for 7 days. In contrast, the majority of control embryoid bodies were fully cavitated after 7 days (Shaohua Li, Robert Wood Johnson Medical School, personal communication).

To investigate whether AIF is required for normal cell death at a later stage of embryogenesis, we examined *Aif* null embryos at approximately E8.5 [8–9 somite stage (som)] when normal embryos display cell death at the junction of the neural plate and surface ectoderm during neural tube closure. *Aif* null embryos collected at this stage lacked AIF protein, as shown by Western blot analysis of *Aif* null embryos at an earlier stage (0 som; Fig. 1 *B* and *C*), and were morphologically indistinguishable from their wild-type littermates. We observed a similar distribution of TUNEL-positive cells in wild-type and *Aif* null embryos (Fig. 1 *F–I*), demonstrating that, at this stage, normal apoptotic cell death can occur in the absence of AIF.

Loss of *Aif* Function Causes Extensive Cell Death Beginning at E9, but Embryonic Patterning Is Normal. By E9, *Aif* null embryos were distinguishable from their wild-type littermates. Although still grossly normal, the size of the anterior brain and somites was slightly reduced (Fig. 2*A*). With increasing gestational age, these

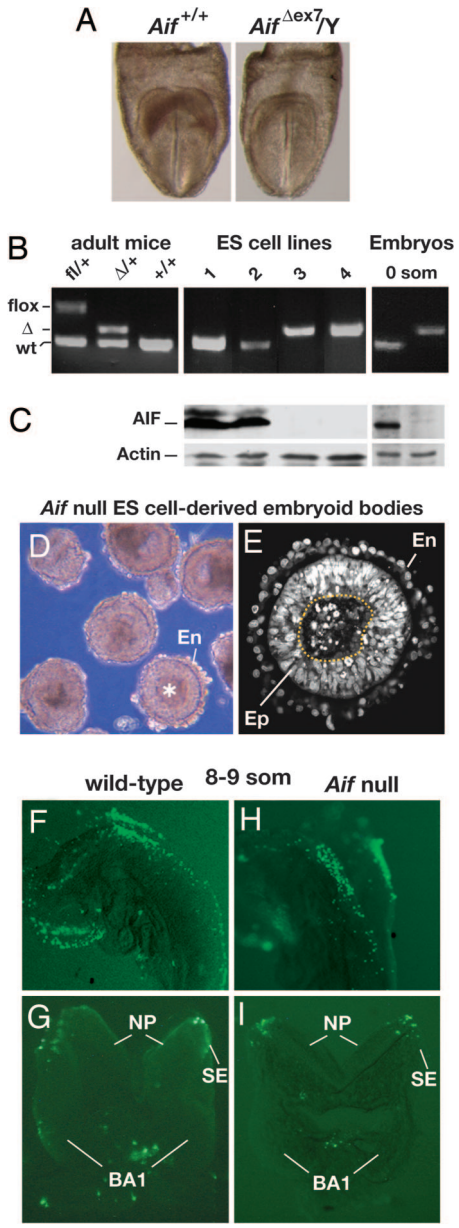

Fig. 1. *Aif* is not required for normal apoptosis during cystic embryoid body formation *in vitro* or neural tube closure in mouse embryos. (*A*) An *Aif*$^{\Delta ex7}$/Y embryo (*Right*), which inherited an *Aif* null allele, and its wild-type littermate (*Left*) at the head fold stage (approximately E7.75). (*B*) PCR genotyping of *Aif* alleles in adult female mice, in ES cell lines derived from wild-type (lines 1 and 2) or *Aif* null (lines 3 and 4) embryos, and in individual wild-type (*Left*) and *Aif* null (*Right*) embryos at the late head fold stage before somites have developed (0 som). (*C*) Immunoblot assay for AIF and actin proteins in lysates of ES cells and 0 som embryos (3 embryos per sample). (*D*) Culture of embryoid bodies formed by *Aif* null ES cells (cell line 3). An outer endodermal cell layer (En) as well as a centrally located cavity (asterisk) are visible. (*E*) Confocal image of a section through an *Aif* null embryoid body (cell line 3) stained with Sytox Green. A dotted line demarcates the centrally located cavity containing pycnotic nuclei of dying cells, which is surrounded by a well-organized pseudostratified columnar epithelium (Ep). The presence of this layer indicates that processes typical of early postimplantation mouse development have occurred in the interior of the embryoid bodies and that the death of cells in the center was the outcome of a developmentally regulated process (1). (*F–I*) Lateral and dorsolateral views of wild-type and *Aif* null 8- to 9-som embryos, respectively, assayed for cell death by TUNEL staining in whole mount (anterior is to the left) (*F* and *H*) or in transverse vibratome sections at the level of the first branchial arch (BA1) (*G* and *I*). Note the TUNEL-positive cells localized at the junction between the neural plate (NP) and surface ectoderm (SE), a region where apoptosis normally occurs as the neural tube is closing.

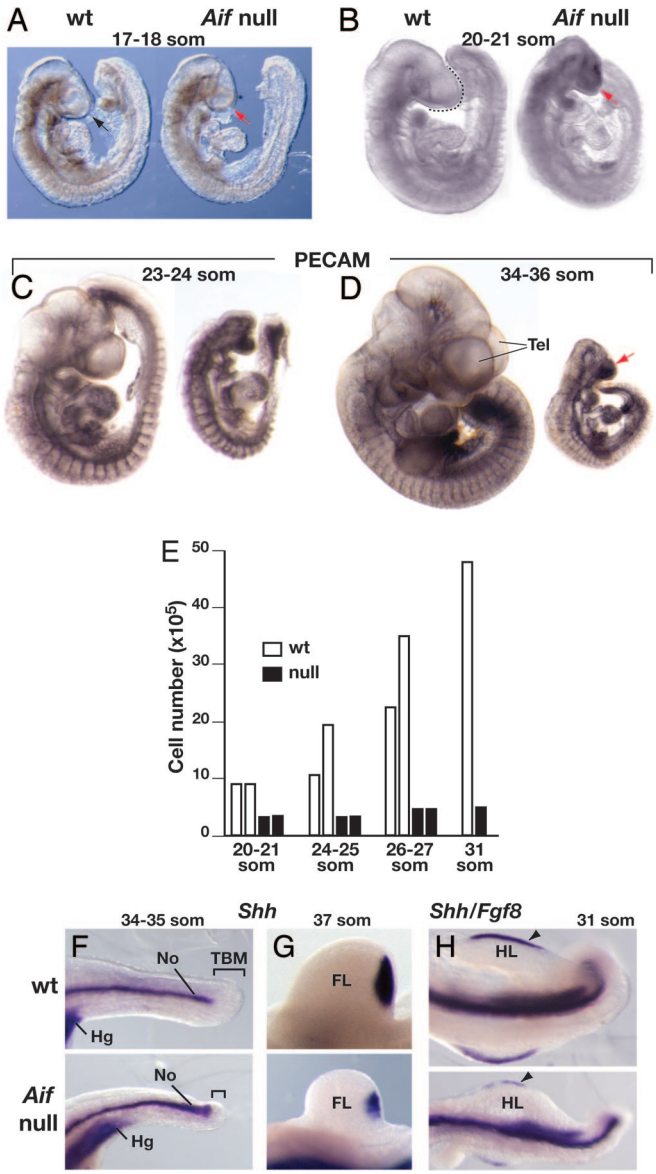

Fig. 2. Loss of *Aif* function impairs embryo growth but not patterning. (*A–D*) Comparison of *Aif* null and wild-type embryos at the somite stages indicated. Littermates are shown in *A*, *B*, and *D*. Embryos in *C* and *D* were stained with an antibody against platelet/endothelial cell adhesion molecule to mark the developing blood vessels. The black arrow and black dotted line in *A* and *B*, respectively, indicate the forebrain in wild-type embryos. The telencephalic vesicles (Tel) are indicated in *D*. The red arrows point to the reduced forebrain/Tel in *Aif* null embryos. (*E*) Wild-type and *Aif* null embryos at the somite stages indicated were disaggregated, and the cell number was counted. Each bar shows the number of cells in an individual embryo. (*F–H*) Whole mount *in situ* hybridization with the probe(s) indicated on embryos at the somite stages indicated. Wild-type and mutant embryos are shown at the same magnification. In all panels, anterior/rostral is to the left and posterior/caudal is to the right. Note that the notochord (No) extends along the same proportion (≈85%) of tail length [from the caudal end of the hindgut (Hg), which expresses *Shh*, to the tip of the tail] in wild-type and *Aif* null embryos. The tail bud mesenchyme (TBM), which produces progenitors of somites and other tissues, is localized in the region between the caudal end of the notochord and tip of the tail (brackets in *F*). Note also that forelimb (FL) buds in *Aif* null mutants express *Shh* in the posterior mesenchyme (*G*) and that hindimb (HL) buds with an apical ectodermal ridge marked by *Fgf8* expression (arrowhead) form in *Aif* null embryos (*H*).

differences became more pronounced, and *Aif* null embryos were markedly smaller than wild-type embryos at the same somite stage (Fig. 2 *B–D*). By approximately E11.5, the few *Aif* null embryos examined were moribund. To determine the cause of the size difference, we collected somite stage-matched *Aif* null and wild-type embryos, dissociated them, and determined the total cell number per embryo. *Aif* null embryos at 20–21 som contained only ≈1/3 as many cells as their wild-type littermates. Over the next 10 soms (≈20 h), the total cell number in *Aif* null embryos increased by only ≈40%, compared with ≈500% in their wild-type littermates (Fig. 2*E*). Visual inspection of cells from dissociated embryos and forward scatter analysis indicated that cells from the mutant embryos were similar in size (diameter) to normal cells (data not shown). Thus the small size of *Aif* null embryos appears to be due primarily to lower cell number.

Table 1. Mean number of somite pairs (± SD) of embryos harvested at various days of gestation from a cross yielding both *Aif* null and wild-type embryos

	No. of somite pairs	
Embryonic day	WT	*Aif* null
E8.5	11.3 ± 1.9 (n = 30)	8.2 ± 1.7 (n = 13)
E9.0	19.7 ± 4.6 (n = 16)	18.7 ± 4.1 (n = 7)
E9.5	26.3 ± 2.9 (n = 22)	25.0 ± 3.0 (n = 6)
E10.5	38.2 ± 3.0 (n = 17)	37.7 ± 2.8 (n = 10)

Despite their markedly reduced cell number (10-fold lower than normal at 30–31 som), patterning of *Aif* null embryos was only slightly delayed. Although the region where somite progenitors arise was substantially reduced in *Aif* null as compared with wild-type embryos (Fig. 2 *C*, *D*, and *F*), somitogenesis lagged by only 2–3 h. Thus, *Aif* null embryos had only 1–2 fewer somite pairs than their wild-type littermates up to at least E10.5 (38 som) (Fig. 2 *B–D* and Table 1). Notochord, as marked by *Shh* expression, continued to form posteriorly and, as in wild-type embryos, extended along ≈85% of the length of the tail in *Aif* null embryos at 34–35 som (Fig. 2*F*). Other tissues, including vasculature, as marked by staining for platelet/endothelial cell adhesion molecule (Fig. 2 *C* and *D*), and limb buds (Fig. 2 *G* and *H*) also appeared to form at the normal time. This observation was not unexpected for forelimb buds, because their development normally commences at ≈18 som, a stage when the mutant embryos were only mildly growth retarded. However, it was surprising that hindlimb buds, which normally begin to form at 27 som, also appeared to develop appropriately even though the *Aif* null embryos were severely growth retarded. Thus, the substantial tissue loss that occurs in *Aif* null mutants does not interfere with the temporal progression of embryonic patterning.

To determine why *Aif* null embryos failed to grow, we assayed for BrdU incorporation in various tissues at 20–25 som. No significant difference in the percentage of labeled cells was detected between *Aif* null and wild-type embryos (Table 2), suggesting that a reduced rate of cell proliferation was not the primary cause of the low cell number in *Aif* null embryos. However, assays for TUNEL at 24–25 som showed extensive abnormal cell death in *Aif* null embryos (Fig. 3 *A* and *B*). These observations explain the overall reduced cell number in *Aif* null embryos. It is unclear why abnormal cell death was not detected in mutant embryos at earlier somite stages (e.g., 8–9 som; Fig. 1 *H* and *I*), even though *Aif* was inactivated in all cells by the 64-cell stage and AIF protein was not detected at 0 som (Fig. 1*C* and data not shown).

Loss of *Aif* Function Impairs Mitochondrial RC Complex I (CI) Activity in Early Somite Stage Embryos. One possible explanation for cell death in the absence of AIF is based on findings showing that mitochondrial RC activity is reduced and oxidative phosphorylation (Oxphos) is impaired in AIF-deficient cells (7, 9, 10). We therefore assayed the activities of RC complexes in individual *Aif*

Table 2. Percentage of BrdU-positive cells in sections of the tissues indicated from wild-type and *Aif* null embryos with 20–25 somites.

	% BrdU-positive cells	
Section of tissue	WT	*Aif* null
Heart	45.5	46.7
	39.1	42.9
		29.8
Neural tube	75.0	71.5
	71.9	71.0
	60.5	
	52.4	
Somites	79.1	73.1
	72.6	70.2
	65.4	59.8
	60.0	

Each value was determined by counting between 150 and 2,000 cells in sections of an individual embryo.

null and wild-type embryos at early somite stages, before abnormal cell death was observed. We found that CI activity was significantly reduced in *Aif* null (0.03 ± 0.02) vs. wild-type (0.24 ± 0.09) embryos ($P < 0.001$; Fig. 4*A*), whereas CII+CIII and CIV activities appeared normal at this stage of development (Fig. 5, which is published as supporting information on the PNAS web site). To control for possible differences in the number of mitochondria per cell or cells per embryo (11), we compared the ratios of RC complex activities in individual embryos. The ratio of CI/CIV activities was significantly different in *Aif* null vs. wild-type embryos (0.09 ± 0.05 vs. 0.40 ± 0.20; $P < 0.001$) whereas the ratio of CIV/CII+III activities was not (*Aif* null vs. wild-type embryos, 2.28 ± 0.51 vs. 1.96 ± 0.34) (Fig. 4*B*).

To assess the effects of loss of *Aif* function on RC complex proteins, we immunoblotted extracts of individual embryos at 9–10 som. The levels of the 39-kDa and 30-kDa components of CI were markedly reduced, and the 17-kDa component was modestly reduced in *Aif* null as compared with wild-type embryos. In contrast, the core 2 component of CIII was unaffected (Fig. 4*C*). These data are consistent with the hypothesis that loss of *Aif* function affects mitochondrial RC activity by decreasing CI protein levels (7, 9).

Discussion

AIF is thought to have two independent functions, one within mitochondria and another as a promoter of cell death after its release from mitochondria and translocation to the nucleus. Here we have analyzed the consequences of inactivating *Aif* function at the blastocyst stage, and we found that the main phenotype is increased cell death. Our observation that mitochondrial RC CI activity was compromised before extensive abnormal cell death was detected suggests that impairment of energy metabolism could be the cause of the null mutant phenotype. Abnormal energy metabolism may also explain the inability of *Aif*$^{-}$/Y ES cells to participate in chimera formation (3). Interestingly, the *Aif* null phenotype is considerably milder than that observed when all mitochondrial RC activity is inhibited, as in *Tfam* or cytochrome *c* null embryos, which are severely retarded by E8.5 (12, 13).

Our data are consistent with studies showing that the abnormal cell death in postnatal cerebellum and retina in mice carrying the Harlequin (Hq) mutation is caused by a severe reduction in *Aif* function. Cell death in the Hq mutants was attributed to a role for AIF in controlling cellular levels of antioxidants (14, 15). However, the increase in markers of oxidative stress and other effects observed in Hq mutants might be secondary to impaired mitochondrial respiration, because CI activity and expression of CI subunits is reduced in Hq brain and retina (9). As yet, it is not known how AIF functions to maintain the normal level of RC CI activity and proteins. AIF does not appear to be part of CI when it is isolated by standard procedures, and it does not affect transcription of CI subunits (9).

Although previous studies in cell culture suggested that *Aif* regulates apoptosis in the early mouse embryo (3), we show that both the apoptosis-dependent process of cavitation in embryoid bodies and the apoptosis associated with neural tube closure in early somite stage embryos can occur normally in the absence of AIF. Likewise, in *Caenorhabditis elegans*, there is no evidence from loss of function studies that *wah-1*, the sole AIF homolog, is individually required for apoptosis during embryogenesis. RNA interference experiments have shown that reducing *wah-1* function causes a delay in the appearance of embryonic cell corpses as well as a slower growth rate suggestive of a general developmental delay. However, *wah-1* RNA interference does not affect the number of programmed cell deaths in the anterior pharynx of wild-type embryos, although it does cause a slight trend toward fewer cell deaths in a *ced-3* or *ced-4* mutant background. These results suggest that *wah-1* might have indirect

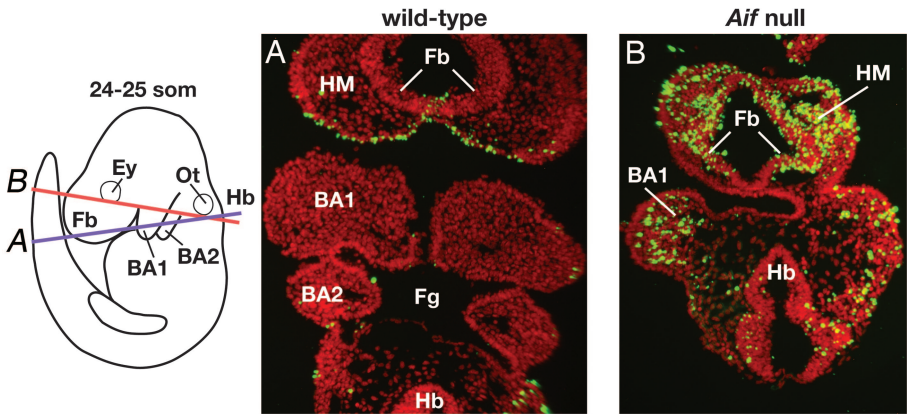

Fig. 3. Loss of *Aif* function causes widespread abnormal embryonic cell death. (*A* and *B*) Coronal sections through wild-type and *Aif* null embryos at 24–25 som assayed for TUNEL (green); nuclei were stained with DAPI (red). The diagram shows the levels at which these sections were taken. The positions of the eye and otocyst are indicated in the diagram; their locations in sections adjacent to those shown were used as landmarks in interpreting the planes of section. Note the large number of TUNEL-positive cells in the forebrain, anterior head mesenchyme, and first branchial arch of the *Aif* null embryo. BA1, first branchial arch; BA2, second branchial arch; Ey, eye; Fb, forebrain; Fg, foregut; Hb, hindbrain; HM, head mesenchyme; Ot, otocyst.

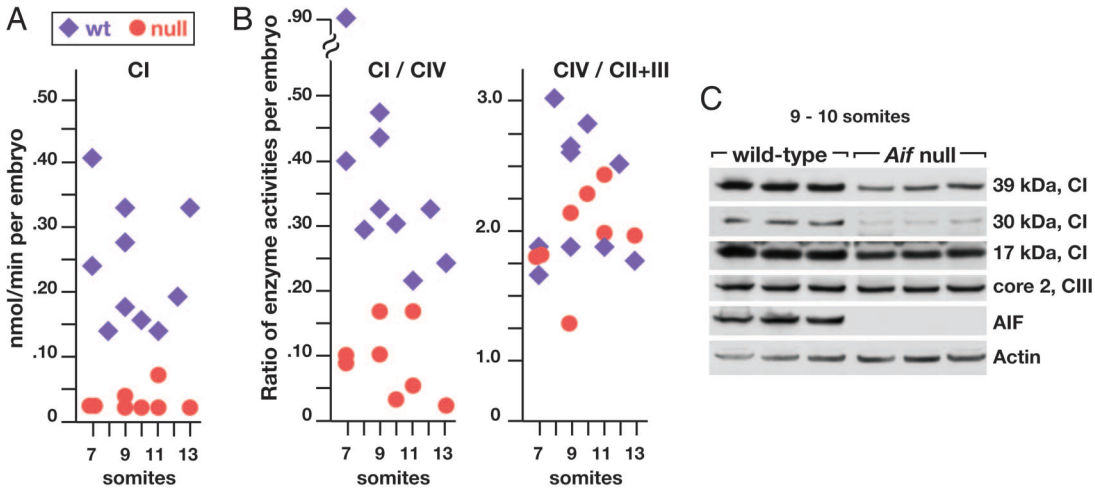

Fig. 4. Loss of *Aif* function impairs RC complex I (CI) activity. (*A*) Comparison of RC CI activity in individual embryos at 7–13 soms. (*B*) Comparison of the ratios of activities of the various RC complexes in individual embryos, showing that reduction of CI activity in individual embryos is not due to differences in cell or mitochondria number. (*C*) Immunoblot assay for respiratory CI proteins in lysates of individual embryos at 9–10 som. Note the significant reduction in the levels of the 39-kDa and 30-kDa proteins of CI in *Aif* null embryos.

interactions with the programmed cell death pathway (16). However, there are loss of function data suggesting that AIF may be required for cell death after certain types of neuronal injury (17). Further analysis is needed to determine whether AIF is an essential mediator of cell death during mouse development or in disease states.

Given the confounding problem that loss of *Aif* function causes extensive cell death in embryos (Fig. 3 and Table 2) and adults (14, 15), such studies may require the use of a mutation that encodes an AIF protein that lacks the presumed apoptogenic function but still has the energy metabolism/antioxidant function (10). This approach has recently been used to demonstrate that cytochrome *c*, a protein also hypothesized to have independent functions in energy metabolism and as a promoter of cell death (6), is required for cell death in some tissues but only late in embryogenesis (18). Interestingly, inactivation of *Apaf1*, caspase 3, or caspase 9 likewise prevents cell death in only some tissues late in embryogenesis (2) and may have no effect on some genetic backgrounds (19, 20), leaving open the question of what genes or combinations of genes are required to promote cell death in the early embryo.

In addition to what our data reveal about *Aif* function in the embryo, they provide a remarkable demonstration of the robustness of the embryonic patterning process. In higher vertebrates such as chickens, mice, and humans, extension of the embryonic body axis occurs in concert with the continuous generation of tissue progenitors at the posterior end of the embryo. Tam and colleagues observed that the rate of somite formation was reduced when they decreased embryo cell number by treating wild-type mouse embryos with an antiproliferative agent at an early stage (21) or by removing a blastomere at the 4-cell stage (22). This observation suggested that the rate of somitogenesis depends on how many progenitor cells are available. In contrast, in mouse embryos homozygous for Amputated, a recessive mutation no longer extant (23), and in *Aif* null embryos, somite formation occurs at the normal rate despite a substantial reduction in the size of the progenitor population, but the somites are much smaller than normal. Furthermore, other tissues in *Aif* null embryos, including notochord, intersomitic blood vessels, and limb buds, also develop on schedule. This finding suggests that the ability to keep normal time irrespective of whether a normal number of progenitor cells is available is a general characteristic of developmental processes, even in systems where organogenesis depends on the continuous generation of progenitor cells.

Methods

Genotyping and Phenotypic Analysis. Genotypes were determined by PCR assays using DNA extracted from ectoplacental cones, yolk sacs, tails, or ES cells as a template. For *Aif* alleles, we used three primers: P1, 5′-TCCCAAACTTCCATTCGGATTTACT-3′; P2, 5′-GAATCTGGAATATGGCACAGAGG-3′; and P3, 5′-GTAGATCAGGTTGGCCAGAAACTC-3′. PCR amplification products were ≈500 bp (flox, P1+P2), 350 bp (wild-type, P1+P2), and 420 bp (Δex7, P2+P3). The presence of the β-Ac-cre transgene was detected by using two primers: 5′-CGACCAGTGTTTGCCTTTTATGG-3′ and 5′-ATTCAACTTGCACCATGCC-3′. Embryos for morphological or histological analysis were collected in cold PBS, fixed in 4% paraformaldehyde, and stored in 70% ethanol at −20°C. Noon of the day when a vaginal plug was detected was considered approximately E0.5. Standard protocols were used for RNA *in situ* hybridizations and staining with a rat anti-platelet/endothelial cell adhesion molecule antibody (553370; BD PharMingen). Cell number per embryo was determined by preparing a single cell suspension from each embryo as described (24) and counting the cells in a hemacytometer. For each embryo, the cell number was determined twice, and the data were averaged.

Cell Proliferation and Apoptosis Assays. For cell proliferation assays, pregnant females were injected i.p. with BrdU at 100 mg/kg body weight, and embryos were collected 1–2 h later. Detection of cells that incorporated BrdU was performed on 5-μm deparaffinized sections by using a BrdU labeling and detection kit (Roche) with the following modifications. Deparaffinized slides were treated with antigen unmasking solution (Vector Laboratories), denatured with 1 M HCl, and permeabilized with proteinase K before incubation with antibody. Slides were counterstained with Sytox Green (Invitrogen) and mounted in Vectashield mounting medium containing DAPI (Vector Laboratories). Cell death was detected on proteinase K-treated 5-μm paraffin or 100-μm vibratome sections as per instructions in the *in situ* cell death detection kit, Fluorescein (Roche).

ES Cell Isolation and Culture. ES cell lines were isolated from individual blastocysts essentially as described (25), except that

knockout serum replacer (no. 10828 028; GIBCO) was substituted for bovine serum (20% vol/vol) and medium conditioned by CHO cells expressing recombinant LIF (Genetics Institute, Cambridge, MA) was added (10% vol/vol) to the culture medium. Once established, ES cell lines were maintained in the undifferentiated state by frequent subculture on mouse embryo fibroblast or STO feeder cells and embryoid body development was obtained as described (1). Embryoid bodies were collected, embedded in plastic, sectioned at 10 μm, and stained with Sytox Green.

Immunoblotting. Western blotting was carried out as described (7) by using antibodies to the C-terminal portion of AIF (AB16501; Chemicon), actin (A-2066; Sigma), cytochrome *c* (PharMingen), and RC CI subunits 39 kDa, 30 kDa, and 20 kDa (all from Molecular Probes).

RC Complex Activities. Assays of RC enzyme activities were performed on digitonin (0.01%; wt/vol) permeabilized cells as described (26). Rotenone-sensitive NADH quinone reductase (CI; EC 1.6.5.3), malonate-sensitive succinate cytochrome *c* reductase (CII+CIII), antimycin-sensitive quinol cytochrome *c* reductase (CIII; EC 1.10.2.2), and cyanide-sensitive cytochrome *c* oxidase (CIV; EC 1.9.3.1) were spectrophotometrically measured by using a dual-wavelength spectrophotometer (DW-2000; SLM–Aminco, Urbana, IL) by using standard procedures (27). The quinone derivative used to measure CIII was decylubiquinol. All measurements were performed at 37°C. Protein levels were determined by the method of Bradford using BSA as a standard. All chemicals were analytical reagent grade from Sigma.

We thank Cori Bargmann, Bruce Edgar, Olivier Pourquie, Cliff Tabin, and Patrick Tam for enlightening discussion; Christina Ahn, Prajakta Ghatpande, and Ariana Nemati for technical assistance; and our colleagues in the Martin laboratory for critical comments on the manuscript. B.D.Y. is the recipient of National Institutes of Health KO8 and American Skin Association awards. This work was supported by research grants from the Association Française contre les Myopathies and the European Union (EUMITOCOMBAT project) (to P.B. and P.R.); Austrian National Bank, Institute of Molecular Biotechnology of the Austrian Academy of Sciences, and European Union (Marie Curie Excellence grant) (to J.M.P.); the Juvenile Diabetes Research Foundation (to M.F.); and the National Institute of Child Health and Human Development (Grant R37-HD25331) (to G.R.M.).

1. Coucouvanis, E. & Martin, G. R. (1995) *Cell* **83,** 279–287.
2. Ranger, A. M., Malynn, B. A. & Korsmeyer, S. J. (2001) *Nat. Genet.* **28,** 113–118.
3. Joza, N., Susin, S. A., Daugas, E., Stanford, W. L., Cho, S. K., Li, C. Y., Sasaki, T., Elia, A. J., Cheng, H. Y., Ravagnan, L., *et al.* (2001) *Nature* **410,** 549–554.
4. Susin, S. A., Lorenzo, H. K., Zamzami, N., Marzo, I., Brenner, C., Larochette, N., Prevost, M. C., Alzari, P. M. & Kroemer, G. (1999) *J. Exp. Med.* **189,** 381–394.
5. Modjtahedi, N., Giordanetto, F., Madeo, F. & Kroemer, G. (2006) *Trends Cell Biol.* **16,** 264–272.
6. Green, D. R. (2005) *Cell* **121,** 671–674.
7. Joza, N., Oudit, G. Y., Brown, D., Bénit, P., Kassiri, Z., Vahsen, N., Benoit, L., Patel, M. M., Nowikovsky, K., Vassault, A., *et al.* (2005) *Mol. Biol. Cell* **25,** 10261–10272.
8. Lewandoski, M., Meyers, E. N. & Martin, G. R. (1997) *Cold Spring Harb. Symp. Quant. Biol.* **62,** 159–168.
9. Vahsen, N., Cande, C., Briere, J. J., Bénit, P., Joza, N., Larochette, N., Mastroberardino, P. G., Pequignot, M. O., Casares, N., Lazar, V., *et al.* (2004) *EMBO J.* **4,** 4679–4689.
10. Urbano, A., Lakshmanan, U., Choo, P. H., Kwan, J. C., Ng, P. Y., Guo, K., Dhakshinamoorthy, S. & Porter, A. (2005) *EMBO J.* **24,** 2815–2826.
11. Chretien, D., Gallego, J., Barrientos, A., Casademont, J., Cardellach, F., Munnich, A., Rotig, A. & Rustin, P. (1998) *Biochem. J.* **329,** 249–254.
12. Larsson, N. G., Wang, J., Wilhelmsson, H., Oldfors, A., Rustin, P., Lewandoski, M., Barsh, G. S. & Clayton, D. A. (1998) *Nat. Genet.* **18,** 231–236.
13. Li, K., Li, Y., Shelton, J. M., Richardson, J. A., Spencer, E., Chen, Z. J., Wang, X. & Williams, R. S. (2000) *Cell* **101,** 389–399.
14. Klein, J. A., Longo-Guess, C. M., Rossmann, M. P., Seburn, K. L., Hurd, R. E., Frankel, W. N., Bronson, R. T. & Ackerman, S. L. (2002) *Nature* **419,** 367–374.
15. Klein, J. A. & Ackerman, S. L. (2003) *J. Clin. Invest.* **111,** 785–793.
16. Wang, X., Yang, C., Chai, J., Shi, Y. & Xue, D. (2002) *Science* **298,** 1587–1592.
17. Cheung, E. C., Melanson-Drapeau, L., Cregan, S. P., Vanderluit, J. L., Ferguson, K. L., McIntosh, W. C., Park, D. S., Bennett, S. A. & Slack, R. S. (2005) *J. Neurosci.* **25,** 1324–1334.
18. Hao, Z., Duncan, G. S., Chang, C. C., Elia, A., Fang, M., Wakeham, A., Okada, H., Calzascia, T., Jang, Y., You-Ten, A., *et al.* (2005) *Cell* **121,** 579–591.
19. Houde, C., Banks, K. G., Coulombe, N., Rasper, D., Grimm, E., Roy, S., Simpson, E. M. & Nicholson, D. W. (2004) *J. Neurosci.* **24,** 9977–9984.
20. Okamoto, H., Shiraishi, H. & Yoshida, H. (2006) *Cell Death Differ.* **13,** 668–671.
21. Tam, P. P. (1981) *J. Embryol. Exp. Morphol.* **65,** 103–128.
22. Power, M. A. & Tam, P. P. (1993) *Anat. Embryol.* **187,** 493–504.
23. Flint, O. P., Ede, D. A., Wilby, O. K. & Proctor, J. (1978) *J. Embryol. Exp. Morphol.* **45,** 189–202.
24. Burns, J. L. & Hassan, A. B. (2001) *Development (Cambridge, U.K.)* **128,** 3819–3830.
25. Robertson, E. J. (1987) in *Teratocarcinomas and Embryonic Stem Cells*, ed. Robertson, E. J. (IRL, Oxford), pp. 71–112.
26. Chretien, D., Bénit, P., Chol, M., Lebon, S., Rotig, A., Munnich, A. & Rustin, P. (2003) *Biochem. Biophys. Res. Commun.* **301,** 222–224.
27. Rustin, P., Chretien, D., Bourgeron, T., Gerard, B., Rotig, A., Saudubray, J. M. & Munnich, A. (1994) *Clin. Chim. Acta* **228,** 35–51.